

Synthesis and Characterization of Electron-accepting Nonsubstituted Tetraazaacene Derivatives

Kyosuke Isoda,^{*1} Masaharu Nakamura,² Toshinori Tatenuma,¹ Hironori Ogata,³ Tomoaki Sugaya,¹ and Makoto Tadokoro^{*1}

¹Department of Chemistry, Faculty of Science, Tokyo University of Science, 1-3 Kagurazaka, Shinjuku-ku, Tokyo 162-8601

²Department of Chemistry, Graduate School of Science, Osaka City University, Sugimoto-cho, Sumiyoshi-ku, Osaka 558-8585

³Department of Materials Chemistry, College of Engineering, Hosei University, Koganei, Tokyo 184-8584

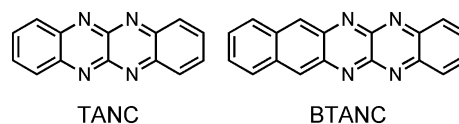
(Received May 24, 2012; CL-120448; E-mail: k-isoda@rs.tus.ac.jp)

Oligoacenes are of interest as organic p-type semiconductors for use in electronic devices, but their use as n-type semiconductors is limited. *N*-Heteroacenes have been investigated as oligoacene-based n-type semiconductors due to their enhanced electron affinity. Herein, we report the synthesis, X-ray crystal structures, electrochemical, and field-effect transistor properties of TANC and BTANC.

Oligoacenes, a class of organic molecules consisting of linearly fused aromatic ring systems, have attracted attention because of their potential as effective carrier-transporting materials in electronic devices.¹ Many p-type organic semiconductors based on oligoacene frameworks such as tetracene,² pentacene,³ and their analogs⁴ have been prepared and studied for their conductive properties. For example, p-type oligoacene-based semiconductors have been investigated as organic hole-transporting layers in organic field-effect transistors (FETs),⁵ as spin-casted films in photovoltaic cells,⁶ and as vacuum-deposited films in a light-emitting diodes.^{4b} In contrast, the number of n-type organic semiconductors based on oligoacene frameworks is still limited, with the exception of perfluorinated oligoacene.⁷

N-Heteroacenes are a type of hetero-oligoacene in which some C atoms have been replaced by N atoms. The introduction of *N*-imino groups to the oligoacene framework makes *N*-heteroacenes good candidates for electron-transporting materials as electron acceptors because *N*-imino groups have a high electron affinity. Molecules possessing the *N*-heteroacene framework are more susceptible to reduction than heteroacenes containing O or S atoms.⁸ Winkler and co-workers have investigated the theoretical properties of *N*-heteroacenes to elucidate their ability to act as n-channel semiconducting or electron-accepting materials.⁹ However, the solubility of *N*-heteroacenes decreases in organic solvent as the number of fused benzene rings in the molecule increases. Therefore, Bunz and co-workers have synthesized highly soluble *N*-heteroacene derivatives by attaching bulky triisopropylsilyl (TIPS) groups to *N*-heteroacene frameworks.^{10a} The *N*-heteroacene derivatives showed high FET behavior owing to rapid electron transport achieved by tuning the molecular arrangements in a thin film, which was achieved despite the presence of bulky substituents.¹⁰ However, unsubstituted *N*-heteroacenes, which have low solubility, are expected to have higher FET activity because high-density stacking between molecules is possible. Moreover, the electron-accepting properties of nonsubstituted *N*-heteroacenes can be tuned by introducing appropriate groups into the *N*-heteroacene frameworks.

Here, we focus on two nonsubstituted, electrochemically stable *N*-heteroacenes with fundamental frameworks. The *N*-heteroacenes TANC (5,6,11,12-tetraazatetracene) and BTANC



Scheme 1. Molecular structures of TANC and BTANC.

(5,6,13,14-tetraazapentacene) are tetraazaacene analogs of tetracene and pentacene, respectively (Scheme 1). These oligoacenes can be purified by sublimation at reduced pressure and they electrochemically generate stable anionic radicals by accepting one electron. TANC and BTANC are expected to function as good semiconductors since their structures are similar to those of tetracene and pentacene, which have remarkable semiconducting properties. In this report, the syntheses, structures, and physical properties of TANC and BTANC, and their FET activities as noble n-type semiconductors are discussed.

BTANC was prepared for this study according to a synthetic procedure similar to that previously reported for TANC.¹¹ BTANC was synthesized by a thermal condensation between 2,3-diaminonaphthalene and 2,3-dichloroquinoxaline in ethylene glycol, followed by oxidation with PbO₂ in CHCl₃. After recrystallization from CHCl₃/hexane, BTANC was obtained as a blackish-green solid in 90% yield. TANC and BTANC were identified by ¹H NMR, ¹³C NMR, and IR spectroscopy, fast atom bombardment (FAB) mass spectrometry, X-ray crystallography, and elemental analysis.

Single crystals of TANC and BTANC were grown from CH₃CN and CHCl₃/hexane (1:2, v/v), respectively.¹² Their molecular structures were revealed by the crystallographic analysis to be approximately planar (Figures 1a and 1c). The crystal structure of TANC is similar to that of tetracene,¹³ with a type of herringbone array of molecules with face-to-edge packing (Figure S1¹⁹). The shortest stacking distance between TANC molecules is C(6)···C(7)* (3.4310(19) Å) along the *a* axis (*: $-x - 1, -y + 1, -z + 2$), in which the average distance of face-to-face stacking is 3.3771(7) Å. The crystal array is reinforced along the *c* axis by complementary, weak, and dual CH···N hydrogen bonds (Figure 1b). The distance of C(2)···N(1)* contact is 3.4824(19) Å (*: $-x, -y + 1, -z + 3$). The BTANC crystal is constructed from one-dimensional columnar structures with slipped stacking along the *b* axis. The closest N···N distance between BTANC molecules is N(1)···N(2)* = 3.592(3) Å (*: $x, y + 1, z$), BTANC molecules in neighboring columns connect to each other through four C–H···N hydrogen bonds, C(15)···N(1)* = 3.519(4) Å and C(17)···N(4)* = 3.517(4) Å (*: $-x + 1, -y - 1, -z + 1$) (Figure 1d). The closest C···C distance for an intermolecular π -stacking interaction between BTANC molecules is C(2)···C(14)* = 3.258(4) Å (*: $-x + 1, -y, -z + 1$), in which

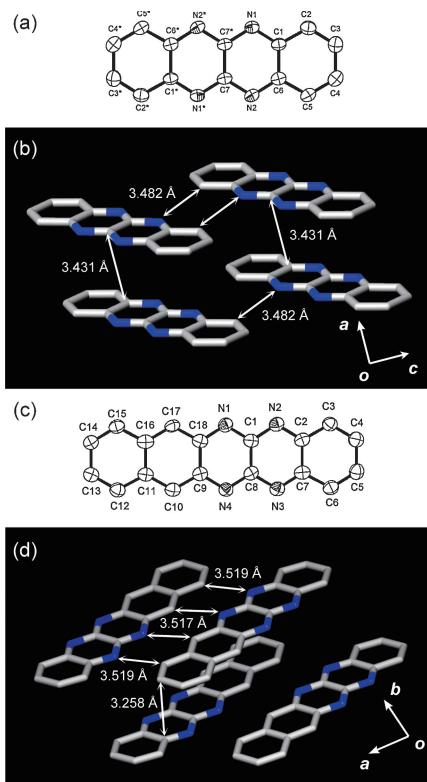


Figure 1. ORTEP drawings and single crystal structures of TANC (a) and (b) and BTANC (c) and (d).

Table 1. Spectroscopic and electrochemical data of TANC and BTANC

	UV-vis absorption λ_{\max}/nm	Redox potential ^a		E_{LUMO}^b /eV	E_g^c /eV
		$E_{1/2}^1$	$E_{1/2}^2$		
BTANC	274, 306, 452	-0.51	-1.09	-4.14	2.68
TANC	260, 414	-0.66	-1.20	-4.00	2.90

^aMeasured by cyclic voltammetry in CH_3CN solution of $n\text{-Bu}_4\text{NPF}_6$ (0.10 M). The redox potential of ferrocene as an internal reference is observed at $E_{1/2}^1 = 0.14$ V. ^b E_{LUMO} is calculated from first half-wave potential ($E_{1/2}^1$) with the assumption that the energy level of ferrocene is -4.8 eV below vacuum level: $E_{\text{LUMO}} = -E_{\text{onset}(\text{red})} - 4.8$ eV. ^cEstimated from the onset position of the UV-vis absorption spectrum in CH_2Cl_2 : $E_g^{\text{opt}} = 1240/\lambda_{\text{onset}}$.

the average distance of the face-to-face stacking is $3.298(3)$ Å, which is less than the sum of the van der Waals radii (3.40 Å) of two C atoms.

The spectroscopic and electrochemical data of TANC and BTANC are summarized in Table 1. The UV-vis spectrum of BTANC in CH_2Cl_2 has an absorption peak at 452 nm, which is bathochromically shifted compared to that of TANC at 414 nm resulting from an expanded aromatic ring system. By expansion of its π -conjugated system, BTANC also had a slight increase in its HOMO energy level (E_{HOMO}) and a decrease in its LUMO energy level (E_{LUMO}) relative to TANC.¹⁴ BTANC also showed a broad absorption band at 602 nm, which is assigned as a weak intramolecular-charge-transfer (CT) interaction between the naphthalene and pyrazinopyradine portions of the molecule.¹⁴

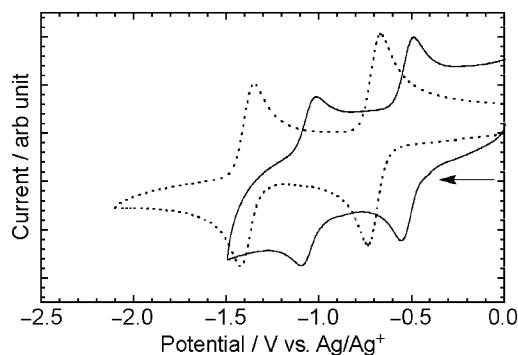


Figure 2. Cyclic voltammograms of TANC (dotted line) and BTANC (solid line) at 1.0 mM in CH_3CN solutions of $n\text{-Bu}_4\text{NPF}_6$ (0.10 M). Sweep rate is 100 mV s^{-1} .

Figure 2 shows the results of the cyclic voltammetry (CV) analyses of TANC and BTANC in CH_3CN solutions of $n\text{-Bu}_4\text{NPF}_6$. BTANC exhibits a reversible two-step and two-electron-transfer peak. The redox potentials of BTANC observed at $E_{1/2}^1 = -0.51$ V and $E_{1/2}^2 = -1.09$ V (vs. Ag/Ag^+) are attributed to the formation of an anionic radical and a dianion, respectively. The $E_{1/2}^1$ of BTANC is less negative than that of TANC ($E_{1/2}^1 = -0.66$ V vs. Ag/Ag^+) due to the stabilization of E_{LUMO} . The E_{LUMO} and E_{HOMO} values of TANC and BTANC were estimated from the redox potential $E_{1/2}^1$ in the cyclic voltammograms and from the absorption edges of the UV-vis spectra. Since E_{LUMO} of TANC (-4.00 eV) and BTANC (-4.14 eV) are lower than those of typical organic electron acceptors such as C_{60} fullerene¹⁵ and perylene diimides,¹⁶ TANC and BTANC should be functional as electron-transporting materials. Furthermore, substituted TANC derivatives have been already reported to be higher electron acceptors rather than nonsubstituted TANC.¹⁷

The organic FET activity of TANC and BTANC was observed using their vapor-deposited thin films on p-doped Si/SiO_2 substrates prepared by high-vacuum evaporation using top-contact geometry at room temperature. It is important to note that the FET activities of TANC and BTANC had to be measured within 30 min of forming the vapor-deposited thin films. Beyond this period of time, electric current could not flow in the thin films because of the formation of noncontacted crystal domains. Analysis of the thin films revealed that both TANC and BTANC functioned as n-type semiconductors as shown in Figure 3. The channel current, I_D , increases according to an increase in V_G , indicating that the thin films behave as n-type semiconductors.^{1a,14} The field-effect mobility of TANC was calculated as $8.9 \times 10^{-5} \text{ cm}^2 \text{ V}^{-1} \text{ s}^{-1}$ with a threshold voltage of 23 V, and an on/off ratio of 90. The field-effect mobility of BTANC was calculated as $3.8 \times 10^{-4} \text{ cm}^2 \text{ V}^{-1} \text{ s}^{-1}$ with a threshold voltage of 27 V, and an on/off ratio of 8×10^2 .

In conclusion, we have investigated the syntheses and crystal structures of TANC and BTANC as two nonsubstituted *N*-heteroacenes that are structurally similar to tetracene and pentacene, respectively. The electrochemical properties of TANC and BTANC were analyzed using CV and their electron-transporting properties were studied in FET analyses. The two *N*-heteroacenes behaved as electron acceptors functioning as novel n-type semiconductors with weaker FET activity

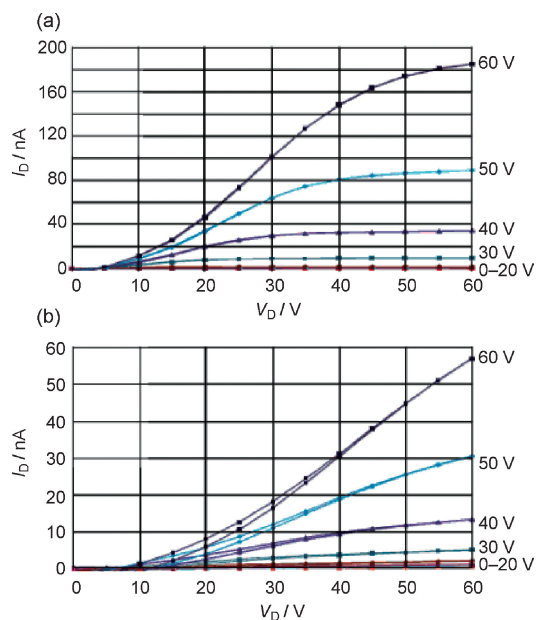


Figure 3. FET characteristics for the thin-films of (a) BTANC and (b) TANC. Gate voltages V_G were applied from 0 to 60 V in increments of 10 V.

compared to n-type semiconductors which have been previously investigated.¹⁸ Although the FET activities of TANC and BTANC are lower than those of tetracene and pentacene, the improvement of their activity is underway by preparing thin films containing less grain boundary in the crystal domains. In the future, the semiconducting activity of TANC, BTANC, and other tetraazaacenes can be improved by introducing electron-donating or electron-accepting substituents, and changing the number of aromatic rings and N atoms in the structures.

This work was supported partially by a Grant-in-Aid for Young Scientists (B, No. 20568620, K.I.) from the Ministry of Education, Culture, Sports, Science and Technology of Japan; Hitachi Metals·Material Science Foundation (K.I.); The Ogasawara Foundation for the Promotion of Science and Engineering (K.I.). We also thank Mitsubishi Chemical Group Science and Technology for help with FET measurements.

References and Notes

- a) J. E. Anthony, *Chem. Rev.* **2006**, *106*, 5028. b) J. E. Anthony, *Angew. Chem., Int. Ed.* **2008**, *47*, 452. c) Y. Cao, M. L. Steigerwald, C. Nuckolls, X. Guo, *Adv. Mater.* **2010**, *22*, 20. d) V. Coropceanu, M. Malagoli, D. A. da Silva Filho, N. E. Gruhn, T. G. Bill, J. L. Brédas, *Phys. Rev. Lett.* **2002**, *89*, 275503. e) M. Bendikov, F. Wudl, D. F. Perepichka, *Chem. Rev.* **2004**, *104*, 4891.
- D. J. Gundlach, J. A. Nichols, L. Zhou, T. N. Jackson, *Appl. Phys. Lett.* **2002**, *80*, 2925.
- a) D. J. Gundlach, Y. Y. Lin, T. N. Jackson, S. F. Nelson, D. G. Schlom, *IEEE Electron Device Lett.* **1997**, *18*, 87. b) F.-J. Meyer zu Heringdorf, M. C. Reuter, R. M. Tromp, *Nature* **2001**, *412*, 517.
- a) C. D. Sheraw, T. N. Jackson, D. L. Eaton, J. E. Anthony, *Adv. Mater.* **2003**, *15*, 2009. b) P. Coppo, S. G. Yeates, *Adv. Mater.* **2005**, *17*, 3001. c) J. E. Anthony, J. S. Brooks, D. L. Eaton, S. R. Parkin, *J. Am. Chem. Soc.* **2001**, *123*, 9482.
- a) A. R. Murphy, J. M. J. Fréchet, *Chem. Rev.* **2007**, *107*, 1066. b) G. Horowitz, *Adv. Mater.* **1998**, *10*, 365.
- a) B. Walker, C. Kim, T.-Q. Nguyen, *Chem. Mater.* **2011**, *23*, 470. b) A. C. Mayer, M. T. Lloyd, D. J. Herman, T. G. Kasen, G. G. Malliaras, *Appl. Phys. Lett.* **2004**, *85*, 6272. c) S. Yoo, B. Domercq, B. Kippelen, *Appl. Phys. Lett.* **2004**, *85*, 5427.
- Y. Sakamoto, T. Suzuki, M. Kobayashi, Y. Gao, Y. Fukai, Y. Inoue, F. Sato, S. Tokito, *J. Am. Chem. Soc.* **2004**, *126*, 8138.
- U. H. F. Bunz, *Chem.—Eur. J.* **2009**, *15*, 6780.
- M. Winkler, K. N. Houk, *J. Am. Chem. Soc.* **2007**, *129*, 1805.
- a) O. Tverskoy, F. Rominger, A. Peters, H.-J. Himmel, U. H. F. Bunz, *Angew. Chem., Int. Ed.* **2011**, *50*, 3557. b) Z. Liang, Q. Tang, J. Xu, Q. Miao, *Adv. Mater.* **2011**, *23*, 1535. c) Q. Miao, T.-Q. Nguyen, T. Someya, G. B. Blanchet, C. Nuckolls, *J. Am. Chem. Soc.* **2003**, *125*, 10284.
- M. Tadokoro, S. Yasuzuka, M. Nakamura, T. Shinoda, T. Tatenuma, M. Mitsumi, Y. Ozawa, K. Toriumi, H. Yoshino, D. Shiomi, K. Sato, T. Takui, T. Mori, K. Murata, *Angew. Chem., Int. Ed.* **2006**, *45*, 5144.
- Crystal data for TANC: $C_{14}H_8N_4$, $M_r = 232.24$, Monoclinic, space group $P2_1/n$ (No. 14) with $a = 4.710(3) \text{ \AA}$, $b = 14.910(10) \text{ \AA}$, $c = 7.653(5) \text{ \AA}$, $\beta = 94.701(14)^\circ$, $V = 535.6(6) \text{ \AA}^3$, $Z = 2$, $D_{\text{calcd}} = 1.440 \text{ g cm}^{-3}$, 99 parameter, $R_1 = 0.0626$, $wR_2 = 0.1434$, and $GOF = 1.223$ for all 1142 data ($I > 4.00\sigma(I)$); 4360 reflections collected; the minimum and maximum residual electron densities are 0.92 and -0.76 e \AA^{-3} . Crystal data for BTANC: $C_{19}H_{11}Cl_3N_4$, $M_r = 401.68$, Monoclinic, space group $P2_1/c$ (No. 14) with $a = 16.2751(3) \text{ \AA}$, $b = 5.77490(10) \text{ \AA}$, $c = 18.6968(3) \text{ \AA}$, $\beta = 101.7166(8)^\circ$, $V = 1720.64(5) \text{ \AA}^3$, $Z = 4$, $D_{\text{calcd}} = 1.550 \text{ g cm}^{-3}$, 236 parameter, $R_1 = 0.0501$, $wR_2 = 0.0565$, and $GOF = 1.017$ for all 3097 data ($I > 2.00\sigma(I)$); 14964 reflections collected; the minimum and maximum residual electron densities are 1.13 and -1.49 e \AA^{-3} .
- a) J. M. Robertson, V. C. Sinclair, J. Trotter, *Acta Crystallogr.* **1961**, *14*, 697. b) R. B. Campbell, J. M. Robertson, J. Trotter, *Acta Crystallogr.* **1962**, *15*, 289.
- J.-i. Nishida, Naraso, S. Murai, E. Fujiwara, H. Tada, M. Tomura, Y. Yamashita, *Org. Lett.* **2004**, *6*, 2007.
- a) S. Miao, S. M. Brombosz, P. v. R. Schleyer, J. I. Wu, S. Barlow, S. R. Marder, K. I. Hardcastle, U. H. F. Bunz, *J. Am. Chem. Soc.* **2008**, *130*, 7339. b) Q. Xie, E. Pérez-Cordero, L. Echegoyen, *J. Am. Chem. Soc.* **1992**, *114*, 3978.
- Z. An, J. Yu, S. C. Jones, S. Barlow, S. Yoo, B. Domercq, P. Prins, L. D. A. Siebbeles, B. Kippelen, S. R. Marder, *Adv. Mater.* **2005**, *17*, 2580.
- Y. Miura, H. Kawai, K. Fujiwara, T. Suzuki, *Chem. Lett.* **2011**, *40*, 975.
- a) B. A. Jones, A. Facchetti, M. R. Wasielewski, T. J. Marks, *Adv. Funct. Mater.* **2008**, *18*, 1329. b) A. Facchetti, M.-H. Yoon, C. L. Stern, H. E. Katz, T. J. Marks, *Angew. Chem., Int. Ed.* **2003**, *42*, 3900.
- Supporting Information is available electronically on the CSJ-Journal Web site, <http://www.csj.jp/journals/chem-lett/index.html>.